Automated Quantitative Assessment of Retinal Fluid Volumes as Important Biomarkers in Neovascular Age-Related Macular Degeneration

TIARNAN D.L. KEENAN, USHA CHAKRAVARTHY, ANAT LOEWENSTEIN, EMILY Y. CHEW, AND URSULA SCHMIDT-ERFURTH

• PURPOSE: To evaluate retinal fluid volume data extracted from optical coherence tomography (OCT) scans by artificial intelligence algorithms in the treatment of neovascular age-related macular degeneration (NV-AMD).

• DESIGN: Perspective.

• METHODS: A review was performed of retinal image repository datasets from diverse clinical settings. SETTINGS: Clinical trial (HARBOR) and trial follow-on (Age-Related Eye Disease Study 2 10-year Follow-On); real-world (Belfast and Tel-Aviv tertiary centers). PATIENTS: 24,362 scans of 1,095 eyes (HARBOR); 4,673 of 880 (Belfast); 1,470 of 132 (Tel-Aviv); 511 of 511 (Age-Related Eye Disease Study 2 10-year Follow-On). OBSERVATION PROCEDURES: Vienna Fluid Monitor or Notal OCT Analyzer applied to macular cube scans. OUTCOME MEASURES: Intraretinal fluid (IRF), subretinal fluid (SRF), and pigment epithelial detachment (PED) volumes.

• RESULTS: The fluid volumes measured in neovascular AMD were expressed efficiently in nanoliters. Large ranges that differed by population were observed at the treatment-naïve stage: 0-3,435 nL (IRF), 0-5,018 nL (SRF), and 0-10,022 nL (PED). Mean volumes decreased rapidly and consistently with anti-vascular endothelial growth factor therapy. During maintenance therapy, mean IRF volumes were highest in Tel-Aviv (100 nL), lower in Belfast and HARBOR-Pro Re Nata, and lowest in HARBOR-monthly (21 nL). Mean SRF volumes were low in all: 30 nL (HARBOR-monthly) and 48-49 nL (others).

• CONCLUSIONS: Quantitative measures of IRF, SRF, and PED are important biomarkers in NV-AMD. Accurate volumes can be extracted efficiently from OCT scans by artificial intelligence algorithms to guide the treatment of exudative macular diseases. Automated fluid monitoring identifies fluid characteristics in different NV-AMD populations at baseline and during follow-up. For consistency between studies, we propose the nanoliter as a convenient unit. We explore the advantages of using these quantitative metrics in clinical practice and research. (Am J Ophthalmol 2021;224:267–281. Published by Elsevier Inc.)

Accepted for publication Dec 10, 2020.

From the Division of Epidemiology and Clinical Applications, National Eye Institute, National Institutes of Health, Bethesda, Maryland, USA (T.D.L.K., E.Y.C.), Centre for Experimental Medicine, Dentistry and Biomedical Sciences, Queen's University of Belfast, Belfast, United Kingdom (U.C.), Tel Aviv Medical Center, Sackler Faculty of Medicine, Tel Aviv University, Tel Aviv, Israel (A.L), and Department of Ophthalmology and Optometry, Christian Doppler Laboratory for Ophthalmic Image Analyses (OPTIMA), Medical University of Vienna, Vienna, Austria (U.S.-E.).

Inquiries to Tiarnan D.L. Keenan, National Institutes of Health, Building 10, CRC, Room 10D45, 10 Center Dr, MSC 1204, Bethesda, MD 20892-1204, USA; e-mail: tiarnan.keenan@nih.gov

THE DIAGNOSTIC ACCURACY OF OPTICAL COHERENCE TOMOGRAPHY IN RETINAL DISEASE

OPTICAL COHERENCE TOMOGRAPHY (OCT) IS NOW the primary imaging modality for the diagnosis and classification of retinal disease, including the late stages of age-related macular degeneration (AMD). In neovascular AMD, an international group of retinal experts observed that OCT is now often used as the primary imaging modality and proposed a new classification of neovascular AMD, based on OCT; they noted that OCT imaging has greater diagnostic precision than traditional imaging modalities and enables detailed 3-dimensional analysis of the vascular anatomical characteristics in neovascular AMD lesions.[1] The diagnostic value of OCT is also exemplified by its ability to differentiate exudative from nonexudative conditions or stages. This has led to greatly improved recognition of nonexudative (quiescent or subclinical) type 1 neovascular complexes as an important entity in AMD.[1,2]

THE MANAGEMENT AND GUIDANCE OF TREATMENT IN RETINAL DISEASE IS DRIVEN BY OPTICAL COHERENCE TOMOGRAPHY

OCT HAS ENABLED DETAILED 3-DIMENSIONAL LOCALIZATION of intraretinal fluid (IRF), subretinal fluid (SRF), and/or pigment epithelial detachments (PED) in exudative retinal conditions, such as neovascular AMD, diabetic macular edema (DME), and retinal vein occlusion (RVO). This has occurred in parallel with the advent of anti-vascular endothelial growth factor (VEGF) therapy, which is highly effective in decreasing these exudative manifestations. However, the therapeutic effect of anti-VEGF injections is typically transient; the duration of action is variable and difficult to predict, depending on the underlying disease state, ocular VEGF levels, drug pharmacodynamics, and other factors. In this context, retreatment decisions in neovascular AMD are typically driven almost entirely by OCT findings,[3–8] and a detailed comparison of IRF and SRF levels at different time points is essential.

THE INTERPRETATION OF OPTICAL COHERENCE TOMOGRAPHY SCANS AT INDIVIDUAL VISITS AND BETWEEN VISITS

IN ROUTINE CLINICAL PRACTICE, A RETINAL SPECIALIST USUally assesses the presence of IRF, SRF, and PED from OCT scans in a qualitative manner. At any individual visit, the clinician may record qualitative descriptions such as "moderate IRF" or "trace SRF," though this requires thorough inspection of numerous B-scans. The OCT software also generates a heatmap, where the macular thickness is compared spatially with reference values from a normative database. In addition, the software may provide a metric, the central subfield thickness (CSFT), that is, the mean retinal thickness in a 1-mm-radius circle centered on the fovea.

Several problems may arise with these approaches. First, qualitative descriptions such as "moderate IRF" have no external definitions, so are likely to have poor intergrader agreement and intragrader consistency. Indeed, several studies have demonstrated suboptimal agreement between retinal specialists and reading center graders even for the binary assessment of fluid presence or absence.[8–10] Second, comparing macular thickness with values from a normative database causes problems, because macular thickness does not consider retinal fluid and neural tissue separately. For example, an eye with DME but decreased neural tissue (from diabetic neurodegeneration) may appear to have normal macular thickness. Third, CSFT is poor at capturing all the potential information available: it does not distinguish between IRF and SRF, and often fails in the presence of a PED; it does account for neural tissue thickness and ignores macular fluid outside the fovea. A recent quantitative comparison between CSFT and fluid volumes identified by artificial intelligence (AI)-based measurement demonstrated poor correlations, particularly in neovascular AMD.[11]

In many clinical situations, particularly for anti-VEGF retreatment decisions, it is essential to compare OCT scans consistently between sequential visits. To do this, retinal specialists typically use built-in OCT software to compare total macular thickness (with a heatmap showing the extent of change) and/or CSFT. However, because these approaches do not distinguish between IRF and SRF and rely on the assumption that neural tissue thickness remains unchanged, these comparisons can result in erroneous interpretation of disease activity. Also, failure of automated segmentation will introduce errors that can invalidate comparisons between scans.

OPTICAL COHERENCE TOMOGRAPHY AS A TOOL FOR STUDYING OUTCOMES IN CLINICAL RESEARCH

OCT IS AN INTEGRAL ELEMENT IN THE ASSESSMENT OF morphologic outcomes in clinical research, particularly in randomized clinical trials (RCTs). In DRCR.net trials exploring DME treatment options, participant selection and retreatment criteria are based predominantly on OCT findings, as are structural outcome measures. For participant selection, DME that is center-involved or not has been a key eligibility criterion.[12–16] Regarding retreatment criteria, a commonly used OCT criterion has been ≥10% change in CSFT. However, there are few data to support this as a clinically meaningful parameter; interestingly, a post hoc analysis of Protocol T concluded that "changes in CSFT accounted for only a small proportion of the total variation in changes in visual acuity. These findings suggest that CSFT is a poor marker for functional improvement or worsening in treatments for DME."[17] Regarding structural outcome measures, the principal OCT outcome measure is typically mean change in CSFT.[12,14–17]

In neovascular AMD, many reports highlight the importance of distinguishing between retinal fluid localization in the intraretinal and subretinal compartments for informing retreatment decisions and predicting visual outcomes.[18–23] Despite this, many recent trials have continued to use relatively crude or binary OCT outcome measures. For example, in the FLUID study RCT, the OCT outcome measure was mean change in CSFT.[20] Similarly, in the HAWK and HARRIER trials of brolucizumab, the OCT

TABLE 1. Characteristics of Study Eyes in the 4 Datasets

	HARBOR	Belfast	Tel Aviv	AREDS2-10Y
SD-OCT Scans (n) of Eyes (n)	24,362 of 1,095	4,673 of 880	1,470 of 132	511 of 511
Anti-VEGF treatment status	Baseline (treatment-naïve) visits and subsequent visits	Baseline (treatment-naïve) visits and subsequent visits	Baseline (treatment-naïve) visits and subsequent visits	Subsequent visits only (1 per eye)
Inclusion criteria	Subfoveal neovascular AMD	Any neovascular AMD	Any neovascular AMD	Any neovascular AMD
SD-OCT device	Cirrus	Spectralis	Spectralis	Cirrus (n = 178) or Spectralis (n = 333)
Setting	Clinical trial	Real-world	Real-world	Clinical trial follow-on

AMD = age-related macular degeneration; AREDS2-10Y = Age-Related Eye Disease Study 2 10-Year Follow-On; SD-OCT = spectral domain optical coherence tomography; VEGF = vascular endothelial growth factor.

outcome measure was change in CSFT; unusually, IRF, SRF, and sub-retinal pigment epithelium (RPE) fluid were considered separately, but only in binary terms of presence or absence.[24] All of these outcome measures have substantial limitations: some are binary or categorical, with great loss of quantitative data; even for the quantitative measures, considering thickness rather than volume means that volume information is lost. This means that, even at the reading center level, assessments of IRF and SRF are often made using a purely qualitative approach; even when quantitative assessments are made, these often consist of CSFT, retinal thickness separately by Early Treatment Diabetic Retinopathy Study (ETDRS) field, and/or point measurements of linear dimensions (eg, maximum height of SRF). These assessments are laborious, confined to the research setting, and do not capture the great wealth and accuracy of quantitative data available from OCT imaging.

OPTIMIZING OPTICAL COHERENCE TOMOGRAPHY OUTCOMES: AN OBJECTIVE APPROACH

RECENT ADVANCES IN MACHINE LEARNING HAVE RESULTED in the development of software that can process routinely acquired spectral domain optical coherence tomography (SD-OCT) data and precisely determine the location and severity of macular fluid within different tissue compartments.[10,25,26] In this way, the software can automatically generate quantitative metrics related to macular fluid, including IRF, SRF, and PED volumes. As continuous variables, macular IRF and SRF volumes are less susceptible to the problems described above. It is therefore possible that using macular IRF and SRF volumes may provide substantial advantages to research and clinical practice. In structure-function correlations, it is possible that using volume instead of thickness, separating fluid volume from neural tissue volume, distinguishing between IRF and SRF (alongside considering centrality), and monitoring dynamics over time might greatly improve the ability of OCT changes to predict changes in VA.

The purpose of this perspective was to compare AI-acquired volumetric information from available datasets on IRF, SRF, and PED, as these represent biomarkers of interest in the treatment of exudative macular diseases. The specific aims were to identify similarities and differences in the ranges of fluid volumes described in 4 datasets, which were analyzed using 2 different algorithms and obtained during the longitudinal follow-up of patients with neovascular AMD undergoing treatment with anti-VEGF therapy. An additional aim was to ascertain the optimum unit of measurement for IRF and SRF volumes that is appropriate for the spectrum of retinal fluid volumes commonly encountered in this disease.

METHODS

FOR THIS STUDY, 4 SEPARATE DATASETS WITH AI-BASED automated detection and quantification of IRF and SRF volumes were identified. These datasets were examined to identify potential similarities and differences and to describe the ranges of retinal fluid volumes that were reported in representative populations with neovascular AMD. They comprised data from (a) the HARBOR trial,[27] (b) a tertiary referral retinal center in the United Kingdom,[28] (c) a tertiary referral retinal center in Israel,[29] and (d) the AREDS2 10-year Follow-On.[9] The AI algorithm used on the HARBOR trial dataset was the validated algorithm previously published by the University of Vienna,[25] the Vienna Fluid Monitor; the one used on the 3 other datasets was the Notal OCT Analyzer (NOA).[9,10]

• **HARBOR DATASET: LONGITUDINAL OCT DATASET FROM A CLINICAL TRIAL SETTING:** The HARBOR trial (clinicaltrials.gov identifier NCT00891735) was a

multicenter phase III RCT that evaluated the 24-month efficacy of intravitreal ranibizumab 0.5 mg and 2.0 mg administered monthly and on an as-needed basis in neovascular AMD: 1,098 treatment-naïve patients with subfoveal neovascular AMD were recruited at 100 sites in the United States.[30] All patients provided written informed consent, and institutional review board approval was obtained at each center. The inclusion criteria have been described previously.[30] An AI-based fluid analysis of these data using the Vienna AI algorithm has been reported in detail.[27] Study visits included SD-OCT imaging using the Cirrus HD-OCT III (Carl Zeiss Meditec, Dublin, California, USA), with a cube scan comprising 512 A-scans in each of the 128 B-scans, covering a 6 × 6 mm area. All OCT scans were included in the current review, both those obtained at the baseline study visit (treatment-naïve) and at monthly study visits during the 24-month trial period of anti-VEGF therapy.

• **BELFAST HEALTH AND SOCIAL CARE TRUST DATASET: LONGITUDINAL OCT DATASET FROM A REAL-WORLD SETTING:** The Belfast dataset comprised data routinely collected from an electronic medical record system (Medisoft Ophthalmology; Medisoft Limited, Leeds, UK) used for clinical care for neovascular AMD, with the accompanying Spectralis (Heidelberg Engineering, Heidelberg, Germany) SD-OCT data, at this single tertiary referral retinal center.[28] Data relating to the period April 1, 2010, to October 31, 2019, were extracted from the electronic medical record system. The process for using the data in this manner was conducted according to established principles in the United Kingdom National Health Service (The Caldicott Guardian Systems; see systems.hscic.gov.uk/infogov/links/2010cgmanual.pdf). The data guardian gave approval for the use of the anonymized image set, which was exported without any patient identifiers and which adhered to the National Health Service processes and protocols. The inclusion criteria have been described previously.[28] All eyes were treatment-naïve at baseline, were treated with anti-VEGF injection between September 1, 2010, and October 4, 2017, and had at least 2 Spectralis SD-OCT scans in the period between 3 months and 36 months after the first anti-VEGF injection. The patients were treated according to a mixture of Pro Re Nata (PRN) and Treat and Extend regimens. The Spectralis SD-OCT macular cube scans were acquired under standard conditions (31-61 B-scans covering a 6 × 6 mm area). All OCT scans were included in the current review, both those obtained at baseline (treatment-naïve) and during ongoing anti-VEGF treatment.

• **TEL AVIV MEDICAL CENTER DATASET: LONGITUDINAL DATASET FROM A REAL-WORLD SETTING:** The Tel Aviv dataset comprised data routinely collected as part of clinical care for neovascular AMD, with the accompanying Spectralis SD-OCT data, at this single tertiary referral retinal center. Institutional review board approval was obtained, and the research was conducted under the tenets of the Declaration of Helsinki. The inclusion criteria have been described previously.[29] These included the availability of a Spectralis SD-OCT macular cube scan acquired between August 1, 2009, and November 30, 2018. The scans were acquired under standard conditions (31-61 B-scans covering a 6 × 6 mm area). All OCT scans were included in the current review, both those obtained at baseline (treatment-naïve) and during ongoing anti-VEGF treatment. The patients were treated according to a mixture of PRN and Treat and Extend regimens. In individuals with bilateral neovascular AMD, the scans were separated into those from first-treated and second-treated eyes (ie, fellow eyes diagnosed with neovascular AMD during anti-VEGF therapy of the first eye).

• **AGE-RELATED EYE DISEASE STUDY 2 10-YEAR FOLLOW-ON DATASET: CROSS-SECTIONAL (OPPORTUNISTIC) OCT DATASET FROM A FOLLOW-ON TRIAL SETTING:** The AREDS2 was a multicenter phase III RCT that analyzed the effects of nutritional supplements on the course of AMD: 4,203 participants were recruited at 82 retinal clinics in the United States.[31] Institutional review board approval was obtained at each clinical site and written informed consent for the research was obtained from all study participants. The research was conducted under the tenets of the Declaration of Helsinki and complied with the Health Insurance Portability and Accountability Act. The inclusion criteria have been described previously.[31] Following close-out of the main study at 5 years, 709 participants underwent a single repeat evaluation at 10 years. The 10-year Follow-On study visit included SD-OCT imaging of the macula, using either the Cirrus (cube scan comprising 512 A-scans in each of the 128 B-scans covering a 6 × 6 mm area) or Spectralis (high-speed volume scan comprising 97 B-scans, ART 9 [max15] with standard orientation [0°], covering a 20 × 20° area). Analysis of this dataset using the NOA has been reported recently.[9] The dataset used in the current review comprised 511 eyes with neovascular AMD, all of which had previously been treated with anti-VEGF injections (ie, not treatment-naïve).

• **THE NOTAL OCT ANALYZER:** The development of the NOA has been described previously.[10] In brief, a machine learning and image recognition computational technique was used to develop a classifier that distinguishes normal morphologic features from elevated or distorted contours that occur from fluid presence. The process includes 3 steps: (1) delineation of internal limiting membrane and RPE, using several local and global image processing techniques including pixel-graph optimization; (2) candidate fluid-region identification using standard image processing techniques; (3) machine learning feature-based classification of the candidate regions to distinguish true from false fluid

TABLE 2. Mean Fluid Volumes at the Baseline Visit (Treatment-Naïve State)

Dataset	HARBOR		Belfast	Tel Aviv—First Eyes	Tel Aviv—Second Eyes
	Vienna Fluid Monitor				
Algorithm	Monthly	PRN	NOA	NOA	NOA
SD-OCT scans (n)	1,095 (1,095 eyes)		880 (880 eyes)	95 (95 eyes)	37 (37 eyes)
IRF (nL)					
Mean (SD)	122.6 (200.6)	161.0 (224.0)	153.5 (292.5)	311 (643.8)	76.8 (187.6)
Range	0.0-1,458.7	0.0-1,436.9	0.0-2,444.9	0.0-3,435.3	0.0-1,000.2
SRF (nL)					
Mean (SD)	425.4 (563.8)	419.8 (548.8)	179.0 (316.9)	202.8 (357.2)	7.0 (15.9)
Range	0.0-5,017.9	0.0-4,303.4	0.0-3,183.3	0.0-1,728.6	0.0-59.0
PED (nL)					
Mean (SD)	414.8 (466.3)	463.9 (625.0)	787.3 (948.7)	1,026.0 (1,380.1)	610.9 (763.8)
Range	0.0-3,032.3	0.0-5,252.4	0.0-10,022.0	0.0-6,916.2	0.0-4,555.9
Analyzed area (mm^2)	28.3	28.3	30.1	41.5	42.0

IRF = intraretinal fluid; NOA = Notal OCT Analyzer; PED = pigment epithelial detachment; PRN = pro re nata; SD-OCT = spectral domain optical coherence tomography; SRF = subretinal fluid.

regions. The algorithm allows automated detection and quantification of IRF and SRF, when applied to a macular volume scan from Cirrus or Spectralis SD-OCT devices. Validation of this algorithm has been reported previously.[9,10]

• **THE VIENNA AI-BASED FLUID MONITOR:** The development of this deep learning algorithm has been described previously.[25] In brief, semantic segmentation,[32] a method based on convolutional neural networks, was developed to perform mapping from OCT images to pixel-level class labels, following end-to-end training on large quantities of labeled training data. In this way, the algorithm assigns each OCT pixel to a class such as IRF, SRF, or normal tissue. This tool permits automated detection and quantification of IRF and SRF, when applied to a macular volume scan from Cirrus or Spectralis SD-OCT devices. Comprehensive validation of this algorithm has been reported previously.[25] This fluid-based algorithm has been applied successfully to many datasets and disease entities such as neovascular AMD, DME, and RVO, as well as for the prediction of retreatment needs and therapeutic outcomes. An application in a large real-world dataset demonstrated its efficacy in routine clinical data (Gerendas BS, et al. IOVS 2018; 59:ARVO E-Abstract 1621).

Previous studies have compared retinal fluid volumes from the algorithms vs manual measurements.[27] For the Vienna Fluid Monitor, in these previous analyses, the level of agreement between the automated and manual measurements was higher than the level of agreement between the manual measurements from 2 human graders.[27] For the NOA, the correlation coefficients for agreement between the automated and manual measurements were high at 0.95 (Spectralis) and 0.92 (Cirrus).[29]

• **DATA ANALYSIS AND IMAGE VISUALIZATION:** Descriptive statistics (mean, standard deviation, and range) were calculated for IRF, SRF, and PED volumes. This was performed separately for each dataset. In order to facilitate more meaningful comparisons between datasets, these statistics were also calculated separately for (1) baseline/treatment-naïve visits and (2) subsequent visits (during anti-VEGF therapy). Of note, the Age-Related Eye Disease Study 2 10-year Follow-On (AREDS2-10Y) dataset contained subsequent visits only. In addition, graphs were made showing changes over time in the mean fluid volumes for the 3 longitudinal datasets.

A small number of representative eyes were selected to demonstrate a wide range of retinal fluid volumes. This was performed, first, to explore the dynamic range of retinal fluid volumes encountered in active disease, toward selection of a single appropriate unit prefix for volume (eg, nanoliter, picoliter, or millimeter cubed). Second, this was done to demonstrate potential methods of automatically visualizing the retinal fluid (eg, en face heatmaps showing the extent of IRF and SRF separately, and B-scans with color-coding of IRF and SRF), for physician inspection and quality assurance. Statistical analysis was performed using SAS version 9.4 (SAS Institute Inc., Carey, North Carolina, USA).

RESULTS

THE CHARACTERISTICS OF THE STUDY PARTICIPANTS AND eyes in the 4 datasets are shown in Table 1. The number of OCT scans analyzed was 24,362 scans of 1,095 eyes (HARBOR), 4,763 scans of 880 eyes (Belfast), 1,470 scans of 132 eyes (Tel Aviv), and 511 scans of 511 eyes

TABLE 3. Mean Fluid Volumes Across Visits During the Maintenance Phase of Anti-VEGF Therapy

Dataset	HARBOR		Belfast	Tel Aviv (All)	AREDS2-10Y
	Vienna Fluid Monitor				
Algorithm	Monthly	PRN	NOA	NOA	NOA
SD-OCT scans (n)	23,267 (1,095 eyes)		3,793 (880 eyes)	1,338 (132 eyes)	511 (511 eyes)
IRF (nL)					
Mean (SD)	21.3 (158.3)	26.8 (133.6)	47.0 (177.1)	100.0 (286.0)	42.5 (194.9)
Range	0.0-3,791.6	0.0-2,961.3	0.0-4,029.4	0.0-2,983.3	0.0-1,905.7
SRF (nL)					
Mean (SD)	29.8 (119.8)	48.0 (171.4)	48.9 (156.9)	48.1 (188.5)	21.4 (123.2)
Range	0.0-1,665.9	0.0-3,594.9	0.0-2,155.1	0.0-2,352.1	0.0-1,865.6
PED (nL)					
Mean (SD)	159.4 (292.0)	225.7 (380.4)	602.5 (633.3)	718.4 (840.1)	618.2 (637.9)
Range	0.0-6,573.2	0.0-4,842.7	0.0-8,528.8	0.0-7,264.5	0.0-5,775.8
Mean analyzed area (mm^2)	28.3	28.3	31.2	41.9	35.4
Mean follow-up (mo)	24	24	19.3	34.6	N/A

AREDS2-10Y = Age-Related Eye Disease Study 2 10-Year Follow-On, IRF = intraretinal fluid, NOA = Notal OCT Analyzer, PED = pigment epithelial detachment, PRN = pro re nata, SD-OCT = spectral domain optical coherence tomography, SRF = subretinal fluid.

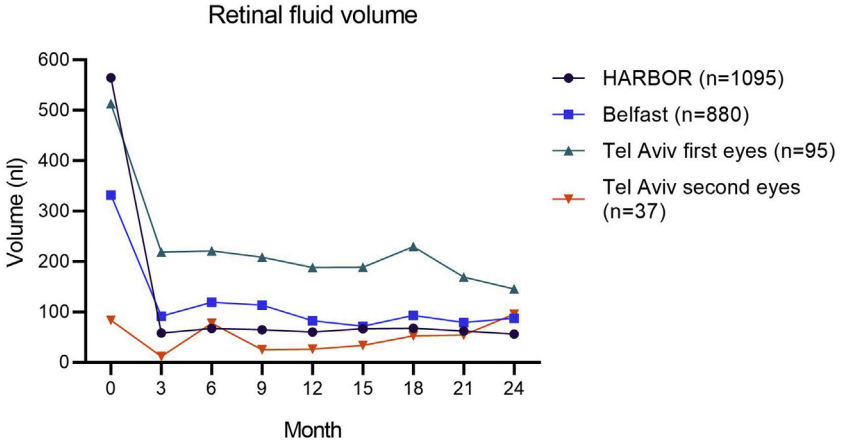

FIGURE 1. Changes over time in retinal fluid volume (sum of intraretinal fluid and subretinal fluid) in the 3 datasets with longitudinal data. The patients in the 2 real-world datasets (Belfast and Tel Aviv) were treated with anti-vascular endothelial growth factor therapy according to a mixture of Pro Re Nata (PRN) and Treat and Extend regimens. Of the patients in the HARBOR clinical trial, half were randomized to monthly and half to PRN treatment. The eligibility criteria also differed between the real-world studies and the clinical trial.

(AREDS2 10-year Follow-On). The proportions of images that did not pass the automated quality filter of the algorithms were 0%, 11%, 14%, and 11%, respectively. As described previously,[9] the NOA rejects images where a reliable assessment of fluid volume is not possible owing to poor image quality, suspected erroneous segmentation, or marked vitreomacular interface abnormalities. The Vienna Fluid Monitor rejects individual A-scans with poor image quality (ie, suspected erroneous internal limiting membrane or RPE delineation), but no entire volume scans in the HARBOR dataset were completely rejected.

The results of the 2 AI-based algorithms are shown in Tables 2 and 3 and Figures 1 and 2. The range of fluid volumes encountered across the spectrum from treatment-naïve neovascular AMD to advanced disease under treatment showed that the most appropriate unit of measurement to encompass the entire dynamic range was the nanoliter (Table 2), as opposed to the microliter (equivalent to the cubic millimeter, mm^3) or picoliter.

• **RETINAL FLUID VOLUMES FROM SCANS AT THE TREATMENT-NAÏVE STAGE:** In all datasets, large ranges of IRF, SRF, and PED volumes were observed in treatment-naïve

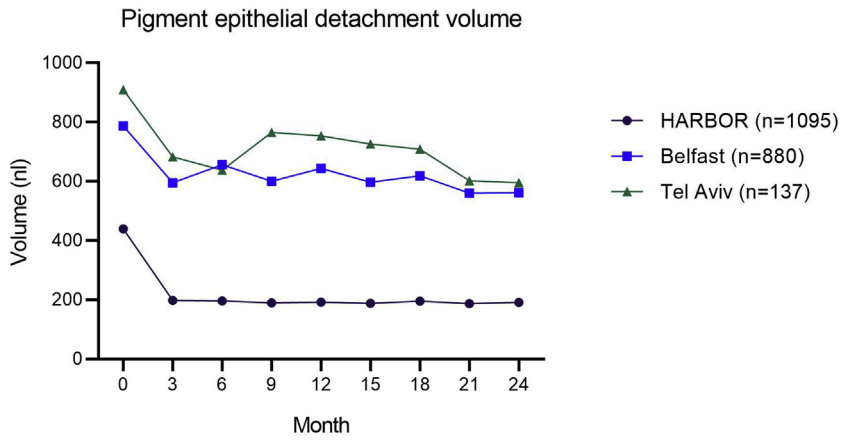

FIGURE 2. Changes over time in pigment epithelial detachment volume in the 3 datasets with longitudinal data. The patients in the 2 real-world datasets (Belfast and Tel Aviv) were treated with anti-vascular endothelial growth factor therapy according to a mixture of Pro Re Nata (PRN) and Treat and Extend regimens. Of the patients in the HARBOR clinical trial, half were randomized to monthly and half to PRN treatment. The eligibility criteria also differed between the real-world studies and the clinical trial.

eyes (Table 2). For example, in the Tel Aviv dataset, IRF volumes ranged from 0 to 3,435 nL, whereas SRF volumes ranged from 0 to 1,729 nL. The mean IRF volume was highest in first-treated eyes in the Tel Aviv dataset (311 nL, standard deviation [SD] 644), lower in the Belfast (154 nL, SD 293) and HARBOR (123 nL, SD 201) datasets, and lowest in second-treated eyes in the Tel Aviv dataset (77 nL, SD 188). A different pattern was observed for SRF: mean SRF volume was highest in the HARBOR dataset (425 nL, SD 564), lower in the Belfast dataset (179 nL, SD 317) and first eyes in the Tel Aviv dataset (203 nL, SD 357), and lowest in second eyes in the Tel Aviv dataset (7 nL, SD 16). Hence, the IRF/SRF volume ratio was highest for the Tel Aviv dataset, intermediate for the Belfast dataset, and lowest for the HARBOR dataset. Regarding PED, the mean volume in the HARBOR dataset (analyzed by the Vienna Fluid Monitor) was 439 nL. In the datasets analyzed by the NOA, the mean PED volume was highest in the first eyes in the Tel Aviv dataset (1,026 nL, SD 1,380), lower in the Belfast dataset (787 nL, SD 949), and lowest in the second eyes in the Tel Aviv dataset (611 nL, SD 764).

• **RETINAL FLUID VOLUMES FROM SCANS DURING ANTI-VEGF THERAPY:** In all datasets, large ranges of IRF, SRF, and PED volumes were observed during anti-VEGF therapy (Table 3). Consistent with previous reports,[27] for all datasets, the mean IRF and SRF volumes decreased rapidly from the baseline visit to subsequent visits (Figure 1). Regarding fluid volumes during the maintenance phase of anti-VEGF therapy, the mean IRF volume was highest in the Tel Aviv dataset (100 nL, SD 286), lower in the Belfast dataset (47 nL, SD 177), and lowest in the HARBOR dataset, particularly for the monthly treatment arm (21 nL, SD 158). For SRF, the mean volumes were similar in the Tel Aviv, Belfast, and HARBOR PRN datasets (48-49 nL for all), but lowest in the HARBOR monthly treatment dataset (30 nL, SD 120). Regarding PED, the mean volume in the HARBOR dataset (analyzed by the Vienna algorithm) was lower in the monthly (159 nL, SD 292) vs PRN (226 nL, SD 380) treatment arm. In the datasets analyzed by the NOA, the mean PED volume was higher in the Tel Aviv dataset (718 nL, SD 840) and lower in the Belfast dataset (603 nL, SD 633).

Changes over time in fluid volumes are shown in Figure 1 (total IRF and SRF) and Figure 2 (PED volume). In most cases, the mean fluid volumes during ongoing anti-VEGF therapy were substantially lower than those observed before starting therapy, for both IRF and SRF. This was particularly true for the HARBOR dataset (likely related to its standardized prospective protocol). The AREDS2-10Y dataset was considered separately, because it comprised fluid volumes obtained at a single visit, where the visits could be at very different time points along the course of neovascular AMD follow-up. The mean volumes were 43 nL (SD 195), 21 nL (SD 123), and 618 nL (SD 638), for IRF, SRF, and PED, respectively.

Regarding the binary detection of retinal fluid presence or absence, error analysis of the NOA was previously reported on the full AREDS2-10Y dataset of 1,127 eyes.[9] The proportions of false-negative and false-positive cases were 5.9% and 9.1%, respectively. Detailed analysis of the false-positive cases showed that, when the NOA falsely predicted that retinal fluid was present, it tended to do this with very low estimated fluid volumes (mean 5.4 nL). Similarly, the false-negative cases tended to be difficult scans (ie, with a high proportion of 44% requiring senior adjudication for fluid presence at the reading center). Error analysis of the Vienna Fluid Monitor was previously reported on a separate dataset of 1,200 OCT scans (including eyes with AMD, DME, and RVO).[25] For the detection of retinal fluid in the AMD cohort, the area under receiver operating curve was 0.93 (IRF) and 0.98 (SRF).

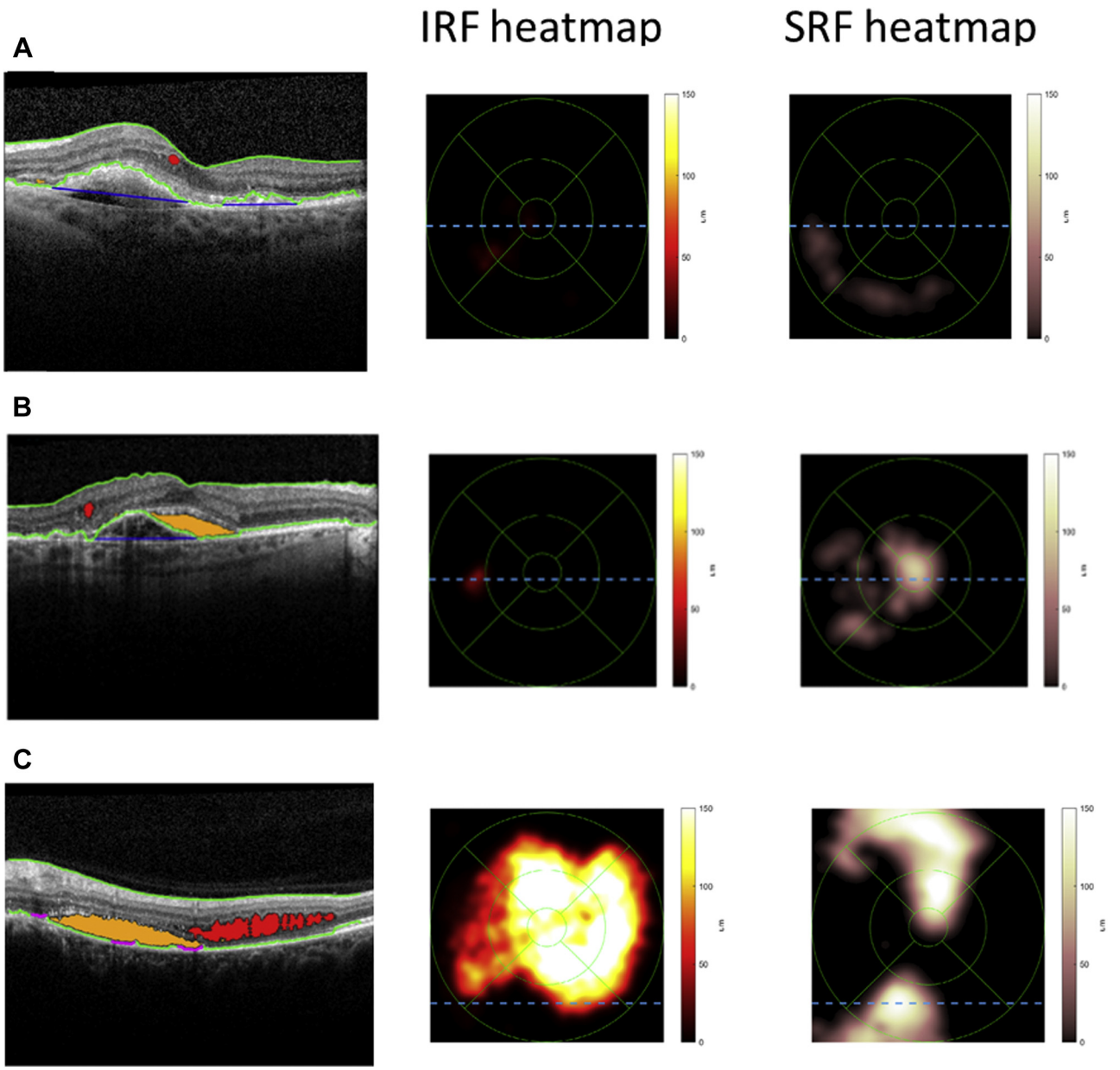

FIGURE 3. Automated detection and quantification of intraretinal fluid (IRF) and subretinal fluid (SRF) by the Notal OCT Analyzer (NOA). Representative examples of Spectralis spectral domain optical coherence tomography scans where the NOA identified the presence of retinal fluid. A representative B-scan is shown in each case, demonstrating how the NOA identifies and color-codes IRF (red) and SRF (orange) on every B-scan. Also shown for each case are the 2 Early Treatment Diabetic Retinopathy Study grid fluid thickness maps, one for IRF and one for SRF; these provide rapid visualization of the location and extent of fluid separately for each tissue compartment. The total volume of IRF and SRF estimated by the NOA is provided in nanoliters (nL). (A) Low total fluid volume (22 nL). (B) Moderate total fluid volume (136 nL). (C) High total fluid volume (3,329 nL).

• **REPRESENTATIVE OPTICAL COHERENCE TOMOGRAPHY SCANS:** Representative SD-OCT scans from eyes with low and high volumes of retinal fluid are shown in Figures 3 and 4. These scans demonstrate how the extent of IRF and SRF visible qualitatively corresponds to quantitative retinal fluid volumes. Figure 3 shows the automated analysis performed by the NOA, whereas Figure 4 demonstrates that performed by the Vienna Fluid Monitor. Both AI algorithms automatically produce 2 heatmaps (overlaid on ETDRS grids), one for IRF and the other for SRF; these show the cross-sectional quantity and spatial extent of the retinal fluid, including the presence or absence of foveal involvement. These provide rapid visualization of the location, extent, and severity of retinal fluid separately for the 2 compartments. For both algorithms, the estimated volumes of IRF and SRF are displayed in nanoliters; these enable precise tracking over time and according to disease and treatment characteristics. In addition, a single representative B-scan is shown in each case, demonstrating how the algorithms identify and separately color-code IRF and SRF on every B-scan in the cube.

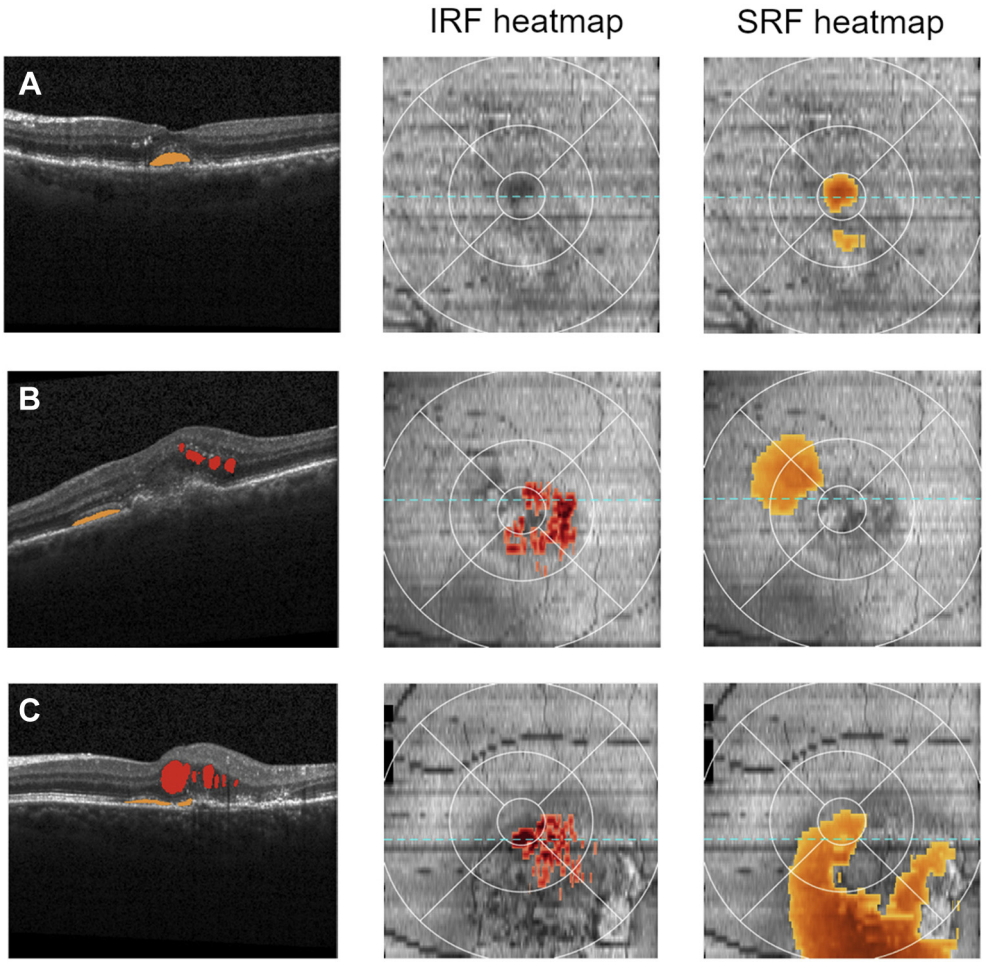

FIGURE 4. Automated detection and quantification of intraretinal fluid (IRF) and subretinal fluid (SRF) by the Vienna Fluid Monitor. Representative examples of Spectralis spectral domain optical coherence tomography scans, where the Vienna algorithm identified the presence of retinal fluid. A representative B-scan is shown in each case, demonstrating how the Vienna algorithm identifies and color-codes IRF (red) and SRF (orange) on every B-scan. Also shown for each case are the 2 Early Treatment Diabetic Retinopathy Study grid fluid thickness maps, one for IRF and one for SRF; these provide rapid visualization of the location and extent of fluid separately for each tissue compartment. The total volume and the volumes of IRF and SRF estimated by the Vienna algorithm are provided in nanoliters (nL). (A) Low total fluid volume (20 nL; IRF = 0 nL, SRF = 20 nL). (B) Moderate total fluid volume (131 nL; IRF = 74 nL, SRF = 57 nL). (C) High total fluid volume (387 nL; IRF = 70 nL, SRF = 317 nL).

DISCUSSION

• **RETINAL FLUID VOLUMES IN DIFFERENT POPULATIONS AND UNDER DIFFERENT TREATMENT REGIMENS IN NEOVASCULAR AGE-RELATED MACULAR DEGENERATION:** We reviewed and compared retinal fluid volume data from datasets obtained in diverse clinical settings. Data were analyzed both at the treatment-naïve and maintenance stages of anti-VEGF therapy. A key feature was the documentation of fluid volumes separately by tissue compartment. We established that the most appropriate unit of measurement was the nanoliter. This unit encompassed the full range of fluid volumes found in the IRF, SRF, and sub-RPE compartments across both treatment-naïve and maintenance stages. It achieved an appropriate balance between the use of decimal places for small volumes and numerous digits for large volumes. Using the same unit of measurement should facilitate easier comparison between different algorithms, datasets, and studies.

A further aim of this review was to identify similarities and differences between the fluid volumes observed in the 4 datasets, which were acquired using 2 commonly available SD-OCT devices and analyzed by 2 different AI algorithms. Regarding the differences in fluid volumes observed at the treatment-naïve stage, plausible explanations include differences in (1) macular neovascularization (MNV) lesion types,[1] (2) earlier or later initiation of anti-VEGF therapy, and (3) other characteristics such as study eligibility criteria. The mean SRF volume at the treatment-naïve visit was greatest in the HARBOR dataset.

Of note, the HARBOR eligibility criteria required best corrected visual acuity of 20/40-20/320 and type 1 or 2 MNV lesions only, where type 1 or mixed 1/2 lesions had to demonstrate activity according to specific criteria.[30] These inclusion criteria likely favored the presence of larger quantities of SRF. By contrast, the relatively high mean IRF volumes and IRF/SRF ratios in the Tel Aviv and Belfast datasets likely reflect the presence of a greater proportion of type 3 MNV lesions in these real-world studies. On segregating first- and second-treated eyes in the Tel Aviv dataset, it was notable that the latter group had the lowest mean IRF and SRF volumes. This finding is consistent with intuition that neovascular AMD in fellow eyes is often diagnosed early, partly owing to frequent OCT monitoring at treatment visits for the first eyes.[33]

A striking finding was the difference in PED volumes between the HARBOR and the 2 real-world datasets, both at the treatment-naïve stage and during maintenance therapy. The mean volumes in the HARBOR dataset were less than half those in the other datasets. Potential reasons for this include the use of different OCT devices, differential recognition of PED boundaries by the 2 algorithms, and genuine differences (related to the patient populations and treatment regimens). Despite potential differences between OCT devices and algorithms, using the same device and algorithm on sequential scans allows fluctuations in PED volume to be captured accurately at the level of individual eyes.

The rapid decrease in fluid volumes observed after the initiation of anti-VEGF therapy has been discussed in detail previously, including in analyses of the HARBOR dataset.[27] The Vienna Fluid Monitor clearly highlighted the sensitivity of the AI-based fluid measurement with respect to drug dosage and type of regimen.[27] Differences in the patterns of fluid resolution and recurrence during the maintenance phase of anti-VEGF therapy were revealed by our analyses. The mean IRF and SRF volumes were generally higher in the real-world datasets, lower in the HARBOR PRN arm, and lowest in the HARBOR monthly arm with the most intensive retreatment. The differences between the clinical trial and real-world results were anticipated, owing to differences in treatment regimens and retreatment criteria. Retreatment criteria are generally less strict in real-world settings, with fewer anti-VEGF injections usually recorded in real-world vs clinical trial settings, reflecting the potential issue of undertreatment in clinical practice worldwide.[30,33,34]

• **IMPORTANCE, IMPLICATIONS, AND POTENTIAL USES IN CLINICAL PRACTICE:** OCT is the primary imaging modality for assessing various aspects of neovascular AMD: diagnosing MNV, identifying the point of conversion from nonexudative to exudative MNV, classifying MNV by lesion type, helping guide prognostic predictions, and assessing the indications for anti-VEGF retreatment.[1,19,27] For most of these tasks, retinal fluid volumes are key biomarkers. Given the increasing prevalence of neovascular AMD, it is therefore very helpful to have software available that can analyze these quantitatively, automatically, and at scale, that is, rapidly, objectively, and consistently.

In clinical practice, the ability to extract quantitative metrics of exudative activity from OCT scans represents an important advance over the qualitative descriptions that are normally used, where retinal fluid is typically graded as present vs absent, or severe vs mild. By avoiding problems of low intragrader consistency and intergrader agreement, this makes it possible to compare exudative activity more meaningfully between sequential and even distant visits of the same individual, or between individuals, irrespective of the physicians' discretion. These quantitative metrics might also lead to improved record-keeping and visualization of exudative activity; the values may be recorded from each visit and lend themselves well to plotting graphs of fluid volume over time (and according to changes in treatment intervals, drugs, and doses).

The application of AI methods allows assessments and comparisons to be made separately for IRF, SRF, and PED. Several studies have already demonstrated that not all exudative activity is equal, in terms of visual prognosis and informing retreatment decisions.[18–23] Notably, the FLUID study aimed to demonstrate that a Treat and Extend approach that tolerated most SRF (assessed manually) achieved noninferior visual outcomes at 2 years, compared with an approach that tolerated neither IRF nor SRF.[20] Indeed, an AI-based approach providing automated quantitative fluid measurements showed no difference between the groups in tolerant vs intolerant SRF reduction (Arnold JJ, et al. IOVS 2019; 60:ARVO E-Abstract 5190). For DME, in a post hoc analysis of the DRCR.net Protocol T, where IRF and SRF were quantified by a fully automated algorithm, aflibercept and ranibizumab were associated with greater reductions of IRF than bevacizumab and IRF was the major factor influencing visual outcomes.[35] Future studies are likely to lead to refined retreatment protocols that may well incorporate more nuanced approaches according to fluid compartment or volume. Adherence to approaches such as this will likely be achieved more easily with the aid of algorithms that identify and quantify fluid types. Overall, in the context of personalized medicine, this may lead to more tailored treatment, ideally so that individuals achieve optimal visual outcomes with as few injections and visits as possible. This might help address some of the shortfall in visual outcomes that has consistently been observed between real-world practice and clinical trials.[33,34,36–39] Of course, assessing this possibility would require prospectively designed trials of standard vs AI-assisted management, as has been performed in other medical fields.[40–42]

There are some clinical scenarios where automated binary detection of retinal fluid presence/absence by itself may be helpful for decisions around retreatment and altered

treatment intervals. We believe that automated quantification will provide additional information that may be very helpful in other clinical scenarios, though this is hypothetical because we are not aware of data directly addressing these questions. For example, the detection of retinal fluid presence by itself may be insufficient for some retinal specialists to recommend treatment/interval change in some circumstances, such as positive but very small quantities of fluid (particularly when the fluid is SRF only, is noncentral, has remained stable over a long period, and/or is assessed to represent nonexudative pathology such as degenerative cysts). If adopted widely, algorithms like this might be used in different ways in different clinical settings (eg, clinical trial vs real-world, or even between different clinics). For example, different clinical trials, clinics, or individual physicians might apply different treatment thresholds. However, an important aim would be for any algorithm to produce volume measurements that were accurate, reliable, and consistent with those from other validated algorithms. In this way, any difference in treatment decisions would arise from physician decision-making rather than inaccuracies from the algorithms themselves.

Other potential uses in clinical practice include helping identify the point of conversion to exudative MNV (including from nonexudative to exudative MNV). Some real-world studies have demonstrated a substantial delay between OCT-defined conversion to exudative MNV and time of first anti-VEGF injection.[43] This is presumably at least partially owing to subtle signs of exudation being missed.

• **POTENTIAL USES IN CLINICAL RESEARCH:** AI algorithms that can automatically identify and quantify retinal fluid volumes may also be very useful in clinical research. In clinical trials, they might be useful at 3 different stages: at recruitment, during study visits, and at endpoints. During recruitment, they could be used to help assess eligibility. For example, particular trials might seek to recruit eyes with SRF only, with retinal volume above or below a certain threshold, or to enrich for type 3 MNV lesions by recruiting many eyes with IRF only. During study visits, they could be used to provide real-time feedback to help assess whether retreatment indications are met, depending on the particular study protocol and its approach to IRF and SRF. At trial endpoints, they could be used to capture the prespecified structural outcome measures. As described above, quantitative metrics for IRF and SRF are likely to have advantages over existing metrics such as CSFT, fluid presence/absence, or maximum height of fluid. They could also be used in post hoc analyses to provide a wealth of data toward the identification of important biomarkers.

Aside from clinical trials, retinal fluid volume quantification may also be useful in other clinical research. They could be used as input and/or output to algorithms (including AI-based ones) that attempt to analyze and predict many aspects of AMD.[19,27,44,45] This includes evaluating factors influencing visual outcomes, influencing retreatment requirements, and characterizing MNV lesion types. In addition, the metrics lend themselves well to structure-function analyses. Analyses that incorporate volumes instead of thicknesses, distinguish between fluid and neural tissue volumes, and consider IRF and SRF separately (including centrality) are likely to yield improved correlations than those from previous attempts. For example, in previous analyses of the HARBOR dataset by the Vienna Fluid Monitor, volume/function correlations demonstrated a negative association between IRF and visual acuity outcome and a weakly positive association between SRF and visual acuity outcome (when the fluid volumes were measured in the central 1 mm diameter).[27] Per unit of 100 nL, an increase in IRF was associated with a visual acuity reduction of 4.0 letters, whereas an increase in SRF was associated with a visual acuity gain of 1.1 letters. More generally, recent studies have already demonstrated the ability of AI approaches to predict visual function from OCT retinal structures, in both geographic atrophy and macular telangiectasia type 2.[46,47] In addition, AI algorithms that identify and quantify nonfluid biomarkers such as hyperreflective foci can help predict the development and local progression of geographic atrophy.[48]

• **STRENGTHS, LIMITATIONS, AND SUGGESTIONS FOR FUTURE RESEARCH:** The strengths of this review included the large size and broad nature of the data included. Importantly, the datasets examined comprised those from both clinical trial settings (with defined eligibility criteria and standardized imaging) and real-world settings (with broad eligibility criteria). In addition, 3 of the datasets included retinal volumes from both treatment-naïve and consecutive treatment stages. Hence, these data encompass the full spectrum of retinal volumes encountered both in routine clinical practice and in clinical trials, both before and during treatment. Additional strengths include the inclusion of data from both Cirrus and Spectralis OCT images and from 2 different AI algorithms.

For optimum use of the algorithms to assess potential changes over time, OCT scans should ideally have consistent foveal centralization and/or registration. If a circular area of retina is analyzed, consistent foveal centralization is sufficient, because ocular torsion will not alter the volumes calculated. If a square area of retina is analyzed, registration is preferable. We also suggest that, for consistency and standardization between algorithms and studies, algorithms should ideally analyze and report 1 or more prespecified macular areas, for example, 6-mm-, 3-mm-, and 1-mm-diameter circles centered on the fovea.

The 2 algorithms described here were not designed to distinguish between hyporeflective spaces representing fluid exudation vs other pathology such as degenerative cysts, tubulations, or cavitations. Although hyporeflective spaces representing nonexudative pathology will be

construed as fluid by the algorithms, any such contributions to the volume measurements are likely to be extremely small and relatively constant over time. Even in clinical situations, the distinction between degenerative cysts and fluid exudation often requires assessment over time and/or response to anti-VEGF treatment. In this context, we contend that the use of algorithms to perform automated assessments of fluid volumes could be very helpful; plotting volumes graphically would demonstrate small volumes that stay relatively stable over time with or without anti-VEGF therapy. In addition, because all areas contributing to fluid measurements are annotated and displayed by the algorithms, reviewing physicians can inspect them for agreement.

The diversity in datasets and treatment regimens in this study makes it difficult to ascribe differences observed between the datasets to specific factors. Also, no data were available where the 2 different algorithms were applied to scans in the same dataset. For this reason, it was not possible to present data related to interalgorithm agreement. Other limitations include the absence of treatment-naïve retinal volumes in the AREDS2-10Y dataset. For these reasons, future research would ideally include any additional AI algorithms and datasets. In particular, applying several AI algorithms to the same dataset would permit calculation of interalgorithm agreement. In the future, it might be possible to create a standardized dataset, comprising OCT scans from various devices, institutions, and clinical/research settings. This would contain a range of pathology considered representative of the full spectrum of neovascular AMD, from several ethnicities, for example, curated according to MNV lesion types 1-3 and lesion maturity. If this dataset had accompanying gold standard retinal volumes obtained by human expert grading, then existing and new AI algorithms could be tested on it, for calibration and comparison with the gold standard and with each other. We also recommend test-retest studies where automated measurements are compared for OCT scans that were acquired sequentially from the same eye (ie, second or minutes apart), in order to verify that the measurements are very similar.

Despite the demonstration from 1 prespecified study that AI-based detection of retinal fluid had higher accuracy and substantially higher sensitivity than detection by retinal specialists in neovascular AMD,[9] we are not aware of any studies designed prospectively to analyze whether AI-based quantification of retinal fluid alters treatment decisions or visual outcomes. We recommend this as an important future area of research.

Another important challenge is to identify a consistent correlation between fluid and function. The goal of anti-VEGF therapy is to improve or at least maintain best corrected visual acuity by resolving retinal fluid as efficiently as possible. Visual loss has been shown to follow a delay in fluid resolution and/or a lower frequency of retreatment.[44] Visual outcomes are highly time-sensitive, so objective fluid monitoring using AI tools will facilitate timely intervention regimens. Gains and losses in visual function are also driven by the specific location of fluid, with several studies providing evidence for a more important role of IRF.[19,20,23] Yet, only the differentiation of fluid compartments by automated segmentation will provide solid evidence for what fluid to target most aggressively during therapy.

The 2 algorithms described here were selected for demonstration purposes. Many other algorithms that perform some form of AI-based retinal fluid detection and quantification have been reported,[49–59] though the majority of these represent proof-of-principle studies only and many of the algorithms have not undergone extensive validation or clinical application. One exception is a deep learning algorithm developed by a collaboration between Moorfields Eye Hospital and DeepMind; in the original study, its main aim was to perform automated referral recommendations for a range of macular pathologies, with automated segmentation of the SD-OCT data into several volumes (including IRF and SRF) as an intermediate step.[26] It has subsequently been applied to a large real-world dataset of treatment-naïve eyes with neovascular AMD.[60]

Aside from the development and robust validation of algorithms like this, other events and factors may be required to bring them to widespread clinical practice. This is analogous to the adoption of OCT technology itself. These events might include early adoption by several specialist academic centers and academic reading centers in a research setting (perhaps including multicenter clinical trials that compare the visual and other outcomes of neovascular AMD with and without automated quantitative assessment of OCT); incorporation within in-built OCT software, to make the technology real-time or near real-time; regulatory approval (eg, FDA approval for software as a medical device and CE marking); increased awareness of the potential advantages of having these data in the clinical community, leading to growing demand; widespread use in many retinal clinics for real-world clinical care.

CONCLUSIONS

QUANTITATIVE MEASURES OF IRF, SRF, AND POTENTIALLY PED are important biomarkers in NV-AMD. We have shown that these can be extracted efficiently and automatically from macular OCT scans by 2 AI-based algorithms, in both clinical trial and real-world settings. In addition to measuring IRF, SRF, and PED volumes, these algorithms produce (1) heatmaps for the visualization of macular fluid severity and extent, separately for IRF and SRF, and (2) annotated B-scans that are color-coded for IRF and SRF, for physician inspection. Automated quantitative measures of retinal fluid volume have substantial

advantages over manual qualitative assessments, for both clinical practice and research. For consistency between studies, we propose the nanoliter as a convenient volumetric unit. These approaches help capture the great wealth of quantitative data available from OCT imaging and should greatly improve the treatment of exudative macular diseases in both real-world practice and clinical trials.

ALL AUTHORS HAVE COMPLETED AND SUBMITTED THE ICMJE FORM FOR DISCLOSURE OF POTENTIAL CONFLICTS OF INTEREST. Funding/Support: This work was supported by intramural program funds from the National Eye Institute, National Institutes of Health (NIH), Department of Health and Human Services, Bethesda, MD. The funding organization participated in the study design; the collection, analysis, and interpretation of data; the writing of the report; and the decision to submit the article for publication. Financial Disclosures: U.C.: consultancy (Alimera, Apellis, Iveric Bio); advisory boards (Bayer, Genentech, Novartis); institutional research support (Bayer, Novartis, Roche); A.L.: consultancy (Allergan, Bayer, Beyeonics, Notal Vision, Novartis, Roche); U.S.-E.: consultancy (Genentech, Kodiak, Novartis, Roche). The rest of the authors have no financial disclosures. All authors attest that they meet the current ICMJE criteria for authorship.

REFERENCES

1. Spaide RF, Jaffe GJ, Sarraf D, et al. Consensus nomenclature for reporting neovascular age-related macular degeneration data: consensus on neovascular age-related macular degeneration nomenclature study group. *Ophthalmology* 2020;127:616–636.
2. Querques G, Srour M, Massamba N, et al. Functional characterization and multimodal imaging of treatment-naive "quiescent" choroidal neovascularization. *Invest Ophthalmol Vis Sci* 2013;54:6886–6892.
3. Chakravarthy U, Pillai N, Syntosi A, Barclay L, Best C, Sagkriotis A. Association between visual acuity, lesion activity markers and retreatment decisions in neovascular age-related macular degeneration. *Eye (Lond)* 2020;34:2249–2256.
4. Schmidt-Erfurth U, Chong V, Loewenstein A, et al. Guidelines for the management of neovascular age-related macular degeneration by the European Society of Retina Specialists (EURETINA). *Br J Ophthalmol* 2014;98:1144–1167.
5. American Academy of Ophthalmology. Age-related macular degeneration preferred practice patterns 2015. Preferred Practice Patterns. Available at: 2019. https://www.aao.org/preferred-practice-pattern/age-related-macular-degeneration-ppp;. Accessed April 25, 2020.
6. Chakravarthy U, Williams M, Group AMDG. The Royal College of Ophthalmologists guidelines on AMD: executive summary. *Eye (Lond)* 2013;27:1429–1431.
7. The National Institute for Health and Care Excellence. Age-related macular degeneration. NICE guideline. Available at: http://www.nice.org.uk/guidance/NG82. Accessed April 13, 2020.
8. Toth CA, Decroos FC, Ying GS, et al. Identification of fluid on optical coherence tomography by treating ophthalmologists versus a reading center in the comparison of age-related macular degeneration treatments trials. *Retina* 2015;35:1303–1314.
9. Keenan TD, Clemons TE, Domalpally A, et al. Retinal specialist vs artificial intelligence detection of retinal fluid from optical coherence tomography: AREDS2 10-year Follow-On. *Ophthalmology* 2021;128:100–109.
10. Chakravarthy U, Goldenberg D, Young G, et al. Automated identification of lesion activity in neovascular age-related macular degeneration. *Ophthalmology* 2016;123:1731–1736.
11. Schmidt-Erfurth U, Pawloff M. Correlation between central retinal thickness and intra-/subretinal fluid volumes measured by deep learning. The Macula Society 43rd Annual Meeting, February 19, 2020, San Diego, California.
12. Baker CW, Glassman AR, Beaulieu WT, et al. Effect of initial management with aflibercept vs laser photocoagulation vs observation on vision loss among patients with diabetic macular edema involving the center of the macula and good visual acuity: a randomized clinical trial. *JAMA* 2019;321:1880–1894.
13. Friedman SM, Almukhtar TH, Baker CW, et al. Topical nepafenec in eyes with noncentral diabetic macular edema. *Retina* 2015;35:944–956.
14. Diabetic Retinopathy Clinical Research N, Wells JA, Glassman AR, Ayala AR, et al. Aflibercept, bevacizumab, or ranibizumab for diabetic macular edema. *N Engl J Med* 2015;372:1193–1203.
15. Diabetic Retinopathy Clinical Research N, Writing C, Aiello LP, Bressler NM, Browning DJ, et al. Rationale for the diabetic retinopathy clinical research network treatment protocol for center-involved diabetic macular edema. *Ophthalmology* 2011;118:e5–e14.
16. Diabetic Retinopathy Clinical Research N, Elman MJ, Aiello LP, Beck RW, et al. Randomized trial evaluating ranibizumab plus prompt or deferred laser or triamcinolone plus prompt laser for diabetic macular edema. *Ophthalmology* 2010;117:1064–1077.e1035.
17. Bressler NM, Odia I, Maguire M, et al. Association between change in visual acuity and change in central subfield thickness during treatment of diabetic macular edema in participants randomized to aflibercept, bevacizumab, or ranibizumab: a post hoc analysis of the protocol t randomized clinical trial. *JAMA Ophthalmol* 2019;137:977–985.
18. Schmidt-Erfurth U, Waldstein SM. A paradigm shift in imaging biomarkers in neovascular age-related macular degeneration. *Prog Retin Eye Res* 2016;50:1–24.
19. Schmidt-Erfurth U, Bogunovic H, Sadeghipour A, et al. Machine learning to analyze the prognostic value of current imaging biomarkers in neovascular age-related macular degeneration. *Ophthalmol Retina* 2018;2:24–30.
20. Guymer RH, Markey CM, McAllister IL, et al. Tolerating subretinal fluid in neovascular age-related macular degeneration treated with ranibizumab using a treat-and-extend regimen: FLUID study 24-month results. *Ophthalmology* 2019;126:723–734.

21. Sharma S, Toth CA, Daniel E, et al. Macular morphology and visual acuity in the second year of the comparison of age-related macular degeneration treatments trials. *Ophthalmology* 2016;123:865–875.
22. Waldstein SM, Simader C, Staurenghi G, et al. Morphology and visual acuity in aflibercept and ranibizumab therapy for neovascular age-related macular degeneration in the VIEW trials. *Ophthalmology* 2016;123:1521–1529.
23. Waldstein SM, Philip AM, Leitner R, et al. Correlation of 3-dimensionally quantified intraretinal and subretinal fluid with visual acuity in neovascular age-related macular degeneration. *JAMA Ophthalmol* 2016;134:182–190.
24. Dugel PU, Koh A, Ogura Y, et al. HAWK and HARRIER: phase 3, multicenter, randomized, double-masked trials of brolucizumab for neovascular age-related macular degeneration. *Ophthalmology* 2020;127:72–84.
25. Schlegl T, Waldstein SM, Bogunovic H, et al. Fully automated detection and quantification of macular fluid in OCT using deep learning. *Ophthalmology* 2018;125:549–558.
26. De Fauw J, Ledsam JR, Romera-Paredes B, et al. Clinically applicable deep learning for diagnosis and referral in retinal disease. *Nat Med* 2018;24:1342–1350.
27. Schmidt-Erfurth U, Vogl WD, Jampol LM, Bogunovic H. Application of automated quantification of fluid volumes to anti-VEGF therapy of neovascular age-related macular degeneration. *Ophthalmology* 2020;127:1211–1219.
28. Chakravarthy U, Havilio M, Syntosi A, Pillai N, Wilkes E, Benyamini G, Best C, Sagkriotis A. Impact of macular fluid volume fluctuations on visual acuity during anti-VEGF therapy in eyes with nAMD. *Eye (Lond)* 2021; https://doi.org/10.1038/s41433-020-01354-4. Online ahead of print.
29. Goldstein M, Havilio M, Rafaeli O, Loewenstein A. A novel AI-based algorithm for quantifying volumes of retinal pathologies in OCT scans. American Academy of Ophthalmology Meeting, October 12, 2019, San Francisco, California, USA.
30. Ho AC, Busbee BG, Regillo CD, et al. Twenty-four-month efficacy and safety of 0.5 mg or 2.0 mg ranibizumab in patients with subfoveal neovascular age-related macular degeneration. *Ophthalmology* 2014;121:2181–2192.
31. AREDS2 Research Group, Chew EY, Clemons T, SanGiovanni JP, et al. The age-related eye disease study 2 (AREDS2): study design and baseline characteristics (AREDS2 report number 1). *Ophthalmology* 2012;119:2282–2289.
32. Noh H, Hong S, Han B. Learning deconvolution network for semantic segmentation. Paper Presented at Proceedings of the IEEE International Conference on Computer Vision. 2015; Santiago de Chile, Chile.
33. Mehta H, Tufail A, Daien V, et al. Real-world outcomes in patients with neovascular age-related macular degeneration treated with intravitreal vascular endothelial growth factor inhibitors. *Prog Retin Eye Res* 2018;65:127–146.
34. Keenan TD, Vitale S, Agron E, et al. Visual acuity outcomes after anti-vascular endothelial growth factor treatment for neovascular age-related macular degeneration: age-related eye disease study 2 report number 19. *Ophthalmol Retina* 2020;4:3–12.
35. Roberts PK, Vogl WD, Gerendas BS, et al. Quantification of fluid resolution and visual acuity gain in patients with diabetic macular edema using deep learning: a post hoc analysis of a randomized controlled trial. *JAMA Ophthalmol* 2020;138:945–953.
36. Rosenfeld PJ, Brown DM, Heier JS, et al. Ranibizumab for neovascular age-related macular degeneration. *N Engl J Med* 2006;355:1419–1431.
37. Brown DM, Michels M, Kaiser PK, Heier JS, Sy JP, Ianchulev T. Ranibizumab versus verteporfin photodynamic therapy for neovascular age-related macular degeneration: two-year results of the ANCHOR study. *Ophthalmology* 2009;116:57–65 e55.
38. Comparison of Age-related Macular Degeneration Treatments Trials (CATT) Research Group, Martin DF, Maguire MG, Fine SL, et al. Ranibizumab and bevacizumab for treatment of neovascular age-related macular degeneration: two-year results. *Ophthalmology* 2012;119:1388–1398.
39. Writing Committee for the UK Age-Related Macular Degeneration EMR Users Group. The neovascular age-related macular degeneration database: multicenter study of 92 976 ranibizumab injections: report 1: visual acuity. *Ophthalmology* 2014;121:1092–1101.
40. Nagendran M, Chen Y, Lovejoy CA, et al. Artificial intelligence versus clinicians: systematic review of design, reporting standards, and claims of deep learning studies. *BMJ* 2020;368:m689.
41. Wang P, Berzin TM, Glissen Brown JR, et al. Real-time automatic detection system increases colonoscopic polyp and adenoma detection rates: a prospective randomised controlled study. *Gut* 2019;68:1813–1819.
42. NIH U.S. National Library of Medicine ClinicalTrials.gov. Breast ultrasound image reviewed with assistance of deep learning algorithms. Available at: http://clinicaltrials.gov/ct2/show/NCT03706534. Accessed May 18, 2020.
43. Yim J, Chopra R, Spitz T, et al. Predicting conversion to wet age-related macular degeneration using deep learning. *Nat Med* 2020;26:892–899.
44. Bogunovic H, Waldstein SM, Schlegl T, et al. Prediction of anti-VEGF treatment requirements in neovascular AMD using a machine learning approach. *Invest Ophthalmol Vis Sci* 2017;58:3240–3248.
45. Jampol LM, Schmidt-Erfurth UM. Clinical practice settings vs clinical trials: is artificial intelligence the answer? [Epub ahead of print]. JAMA Ophthalmol. doi:10.1001/jamaophthalmol.2019.4782.
46. Pfau M, von der Emde L, Dysli C, et al. Determinants of cone and rod functions in geographic atrophy: AI-based structure-function correlation. *Am J Ophthalmol* 2020;217:162–173.
47. Kihara Y, Heeren TFC, Lee CS, et al. Estimating retinal sensitivity using optical coherence tomography with deep-learning algorithms in macular telangiectasia type 2. *JAMA Netw Open* 2019;2:e188029.
48. Schmidt-Erfurth U, Bogunovic H, Grechenig C, et al. Role of deep learning-quantified hyperreflective foci for the prediction of geographic atrophy progression. *Am J Ophthalmol* 2020;216:257–270.
49. Lee H, Kang KE, Chung H, Kim HC. Automated segmentation of lesions including subretinal hyperreflective material in neovascular age-related macular degeneration. *Am J Ophthalmol* 2018;191:64–75.
50. Lee CS, Tyring AJ, Deruyter NP, Wu Y, Rokem A, Lee AY. Deep-learning based, automated segmentation of macular

edema in optical coherence tomography. *Biomed Opt Express* 2017;8:3440–3448.
51. Wang J, Zhang M, Pechauer AD, et al. Automated volumetric segmentation of retinal fluid on optical coherence tomography. *Biomed Opt Express* 2016;7:1577–1589.
52. Xiayu X, Kyungmoo L, Li Z, Sonka M, Abramoff MD. Stratified sampling voxel classification for segmentation of intraretinal and subretinal fluid in longitudinal clinical OCT data. *IEEE Trans Med Imaging* 2015;34:1616–1623.
53. Chiu SJ, Allingham MJ, Mettu PS, Cousins SW, Izatt JA, Farsiu S. Kernel regression based segmentation of optical coherence tomography images with diabetic macular edema. *Biomed Opt Express* 2015;6:1172–1194.
54. Chen X, Zhang L, Sohn EH, et al. Quantification of external limiting membrane disruption caused by diabetic macular edema from SD-OCT. *Invest Ophthalmol Vis Sci* 2012;53:8042–8048.
55. Wilkins GR, Houghton OM, Oldenburg AL. Automated segmentation of intraretinal cystoid fluid in optical coherence tomography. *IEEE Trans Biomed Eng* 2012;59:1109–1114.
56. Fernandez DC. Delineating fluid-filled region boundaries in optical coherence tomography images of the retina. *IEEE Trans Med Imaging* 2005;24:929–945.
57. Venhuizen FG, van Ginneken B, Liefers B, et al. Deep learning approach for the detection and quantification of intraretinal cystoid fluid in multivendor optical coherence tomography. *Biomed Opt Express* 2018;9:1545–1569.
58. Motozawa N, An G, Takagi S, et al. Optical coherence tomography-based deep-learning models for classifying normal and age-related macular degeneration and exudative and non-exudative age-related macular degeneration changes. *Ophthalmol Ther* 2019;8:527–539.
59. Alsaih K, Yusoff MZ, Tang TB, Faye I, Meriaudeau F. Deep learning architectures analysis for age-related macular degeneration segmentation on optical coherence tomography scans. *Comput Methods Programs Biomed* 2020;195:105566.
60. Moraes G, Fu DJ, Wilson M, et al. Quantitative analysis of OCT for neovascular age-related macular degeneration using deep learning [Epub ahead of print]. *Ophthalmology* 2020; https://doi.org/10.1016/j.ophtha.2020.09.025.